ANALYSIS OF N(^{2}D) AND N(^{2}P) EMISSIONS OBSERVED DURING AN ARTIFICIAL AURORAL EXPERIMENT

J. W. Duff
F. Bien

Spectral Sciences, Inc
99 South Bedford Street
Burlington, MA 01803-5169
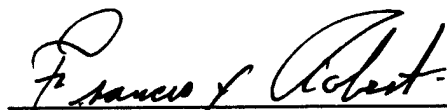
July 1995

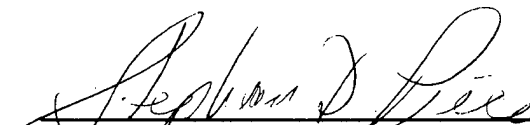Scientific Report No. 2

19960315 064

DTIC QUALITY INSPECTED 1

PHILLIPS LABORATORY
Directorate of Geophysics
AIR FORCE MATERIEL COMMAND
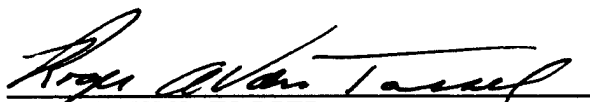**HANSCOM AFB, MA 01731-3010**

This technical report has been reviewed and is approved for publication

FRANCIS X. ROBERT
Contract Manager

STEPHAN D. PRICE
Branch Chief

ROGER VAN TASSEL
Division Director

REPORT DOCUMENTATION PAGE

1. AGENCY USE ONLY (Leave blank)	2. REPORT DATE July 1995	3. REPORT TYPE AND DATES COVERED Scientific Rpt. #2

4. TITLE AND SUBTITLE

Anaysis of $N(^2D)$ and $N(^2P)$ Emissions Observed During an Artificial Auroral Experiment

5. FUNDING NUMBERS

C - F19628-93-C-0052
PE - 62601F
PR - S322
TA - GG
WU - BE

6. AUTHOR(S)

James W. Duff and Fritz Bien

7. PERFORMING ORGANIZATION NAME(S) AND ADDRESS(ES)

Spectral Sciences, Inc.
99 South Bedford Street, #7
Burlington, MA 01803-5169

8. PERFORMING ORGANIZATION REPORT NUMBER

SSI-TR-257

9. SPONSORING/MONITORING AGENCY NAME(S) AND ADDRESS(ES)

Phillips Laboratory
29 Randolph Road
Hanscom AFB, MA 01731-3010

Contract Manager: Frank Robert/GPOB

10. SPONSORING/MONITORING AGENCY REPORT NUMBER

PL-TR-95-2109

11. SUPPLEMENTARY NOTES

12a. DISTRIBUTION/AVAILABILITY STATEMENT

Approved for public release; distribution is unlimited.

12b. DISTRIBUTION CODE

13. ABSTRACT (Maximum 200 words)

The EXCEDE III rocketborne electron beam experiment was successfully launched from White Sands Missile Range on April 27, 1990. An 18 A, 2.4 keV electron beam was pulsed along the Earth's magnetic field lines over an altitude range of 60 to 115 km. Measurements were made of 5200 Å $N(^2D)$, 3466 Å $N(^2P)$, as well as the 3914 Å (0,0) and 5228 Å (0,3) N_2^+ first negative band emissions, between altitudes of 90 to 115 km. A detailed chemical kinetics model describing the interaction of the electron beam with the atmosphere is used to analyze the visible emission from $N(^2D)$ and $N(^2P)$ observed during the EXCEDE III artificial auroral experiment. Quantitative agreement between the model and data is obtained for the $N(^2D)$ column densities. The observed $N(^2P)$ column densities are approximately 50% greater than that predicted by the kinetic model.

14. SUBJECT TERMS

electron beam
artificial aurora
chemical kinetics
nitrogen atoms

15. NUMBER OF PAGES
20

16. PRICE CODE

17. SECURITY CLASSIFICATION OF REPORT UNCLASSIFIED	18. SECURITY CLASSIFICATION OF THIS PAGE UNCLASSIFIED	19. SECURITY CLASSIFICATION OF ABSTRACT UNCLASSIFIED	20. LIMITATION OF ABSTRACT SAR

TABLE OF CONTENTS

LIST OF ILLUSTRATIONS

1. INTRODUCTION

The primary source of NO emissions in an aurorally enhanced upper atmosphere is through odd-nitrogen chemiluminescent reactions involving $N(^4S)$, $N(^2D)$, and $N(^2P)$. Recent papers speculating on the creation of the NO hot bands have identified high energy nitrogen atoms as the source of these emissions. One of the goals of the EXCEDE III measurement program, which has been described previously,[1] is to understand the electron-beam induced infrared fluorescence resulting from chemical reactions and energy transfer processes. To characterize the relative importance of the N atom precursors in NO formation, the $N(^2D)$ and $N(^2P)$ emissions have been measured in EXCEDE III. These measurements are compared to a chemical kinetics model which is tested for consistency by using supporting measurements, such as electron deposition, NO chemiluminescence, and N_2 second positive (2P) emissions. The atomic nitrogen formed when an energetic electron interacts with the atmosphere determines not only how much NO is formed, but the spectral distribution of the chemiluminescence. The relative production of these atoms in a electron excited atmosphere has been measured under controlled conditions in EXCEDE III. Simultaneous measurements of the $^2P \rightarrow {}^4S$, $^2D \rightarrow {}^4S$, and N_2^+ first negative (1N) bands have been performed during this experiment. A carefully controlled electron beam dosing profile gave a direct measure of the odd nitrogen production rates as a function of electron injection. The energy deposition profile was measured using 3914 Å emission, and is well represented by a generalized Gaussian function.[2] Since the exact mission profile was known, the emissions within the field-of-view of each detector could be compared with the chemical kinetics responsible for the nitrogen formation. This report presents an analysis of the nitrogen atoms produced in its two lowest metastable excited states and predicts the amount of $N(^4S)$ formed based on branching ratios reported in the literature.

The instruments used to obtain the N atom concentrations consisted of a visible spectrometer for $N(^2P)$, and dedicated photometer for $N(^2D)$. A second photometer, looking at N_2^+ 1N, was boresighted with each of these instruments. Since several different instruments were used for these measurements, they are described separately in the sections below. In the following sections, we present the measurement of $N(^2D)$ and $N(^2P)$, the modeled concentrations based on the observed N_2^+ (0,0) 1N emissions, and finally a discussion on the comparison.

2. MEASUREMENT OF METASTABLE N(^{2}D) AND N(^{2}P)

2.1 N(^{2}D)

The N(^{2}D) emission was measured by a filter photometer with a center wavelength at 5200 Å and a full width at half maximum (FWHM) of 6.06 Å. The field-of-view (FOV) of the photometer was nominally 6° and was pointed 18° into the afterglow. Data were collected at a sample rate of 750 Hz. In order to correct for possible interfering emission, such as the 0-3 band of the N_2^+ 1N series at 5228 Å or the Herzberg bands of O_2, an additional photometer with a center wavelength at 5228 Å with a FWHM of 5.79 Å was co-aligned with the 5200 Å photometer.

2.2 N(^{2}P)

The measurement of N(^{2}P) produced in EXCEDE III was made by measuring its relative intensity to known features using a visible spectrometer. A more detailed description of this instrument is reported by Reider et al.[2] This instrument had a spectral scan time of 2.8 s. Since alternating scans used a neutral density filter (OD=2) to extend the instrument dynamic range, one 3466 Å measurement was made every 5.6 s. This time, convolved with beam-on times of 7.1 s, limited the number of N(^{2}P) scans to 15, 6 on upleg, one at apogee, and 8 on the downleg. The feature at 3466 Å is in the region of the spectrum where the N_2^+ and N_2 2nd Positive bands are located. In fact, the $\Delta v = 1$ series of N_2(2+) has a band in near coincidence with N(^{2}P), at 3468 Å.

3. CHEMICAL KINETICS MODEL

The most important infrared emitters in an electron-dosed atmosphere include NO, CO_2, NO^+, CO, and O_3. A general chemical kinetics model has been developed to describe the chemical and collisional processes occurring during the dosing of the atmosphere with an energetic electron beam. The model uses a finite rate approach to the modeling of the generation of energy dependent secondary electrons, vibrationally and electronically excited species resulting from collisional energy transfer and chemiluminescent reactions. In particular, time and energy dependent rate equations are solved for arbitrary electron beam dosing to obtain species number densities as a function of time. The secondary electron spectrum is treated by setting up an energy grid (histogram) at sufficiently high resolution to accurately solve electron-molecule and electron-electron interactions. Time-dependent rate equations are then solved for each energy bin. Chemical and collisional processes for individual vibrational states are treated explicitly. Self-relaxation of secondary electrons, which is important due to the high electron beam fluxes produced in the EXCEDE experiment, has been treated by solving the time-dependent Fokker-Planck equation.[3,4] In the remainder of this section, the detailed chemical and collisional processes influencing the production and destruction of metastable nitrogen atoms is discussed in some detail.

When electrons interact with the natural atmosphere, dissociation and ionization form odd nitrogen in the form of $N(^2P)$, $N(^2D)$, and $N(^4S)$. Collisions between these species and O_2 create NO.[5] This production rate is in turn found to be dependent on the ratio of $N(^2D)$ to $N(^4S)$ formed in the interaction of electrons and N_2. Nitric oxide is currently thought to be produced primarily by the reaction of $N(^2D)$ with O_2

$$N(^2D) + O_2 \rightarrow NO + O \tag{1}$$

where the reaction rate constant[6] and NO vibrational distribution[7,8] are well established at room temperature. Recent laboratory studies[8] have indicated that $N(^2P)$ produces NO in high vibrational and rotational states
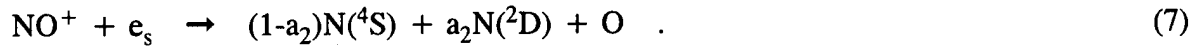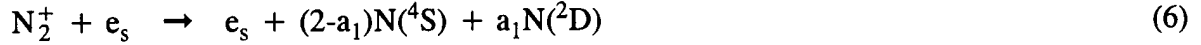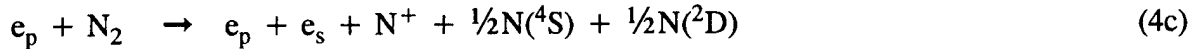
$$N(^2P) + O_2 \rightarrow NO + O \tag{2}$$

with a rate constant a factor of 2 smaller than (1).[6] Furthermore, it has been suggested by Sharma et al.[9] that translationally hot $N(^4S)$ atoms[10] may be a significant source of rotationally hot NO in the thermosphere

$$N(^4S)^* + O_2 \rightarrow NO + O \quad . \tag{3}$$

Although the reaction rate constant and the final vibrational-rotational distribution at high translational energies have not been measured, recent calculations by Duff et al.[11] have established realistic rate constants and NO vibrational-rotational distributions for Reaction (3). A realistic description of the formation and emission of NO in the ambient or auroral atmosphere requires a detailed treatment of nitrogen atom chemistry.

Nitrogen atoms are produced by several major processes; dissociation of N_2 by the primary electrons (e_p) in the electron beam, Reaction (4), dissociation of N_2 by the secondary electrons (e_s) produced by ionization of atmospheric species by the electron beam, Reaction (5), and recombination reactions of the primary ionic products with secondary electrons, Reactions (6) and (7),

$$e_p + N_2 \rightarrow e_p + N(^4S) + N(^2D) \tag{4a}$$

$$e_p + N_2 \rightarrow e_p + N(^4S) + N(^2P) \tag{4b}$$

$$e_p + N_2 \rightarrow e_p + e_s + N^+ + \tfrac{1}{2}N(^4S) + \tfrac{1}{2}N(^2D) \tag{4c}$$

$$e_s + N_2 \rightarrow e_s' + N(^4S) + N(^2D) \tag{5a}$$

$$e_s + N_2 \rightarrow e_s' + N(^4S) + N(^2P) \tag{5b}$$

$$N_2^+ + e_s \rightarrow e_s + (2-a_1)N(^4S) + a_1N(^2D) \tag{6}$$

$$NO^+ + e_s \rightarrow (1-a_2)N(^4S) + a_2N(^2D) + O \quad . \tag{7}$$

The total production rate of N atoms from Reactions (4a) and (4b) is assumed to be $1.5P(N_2^+)$,[12, 13] where $P(N_2^+)$ is the N_2^+ production rate, with the relative formation rate of $N(^2D)$ and $N(^2P)$ in the ratio 0.52:0.48.[14] For dissociative ionization by primary electrons, Reaction (4c), the production rate is $0.50P(N_2^+)$.[15] Thus, the total production rate of N atoms from Reaction (4) is $2P(N_2^+)$, or 1.24 N atoms/ion pair, in good agreement with the results of Porter et al.[12] and Rusch et al.[13] The cross sections for dissociation of N_2 by low energy secondary electrons, Reaction (5), are based on the analysis of Zipf et al.[14] The rate constants for the recombination of N_2^+ and NO^+ ions with secondary electrons, Reactions (6) and (7), have been measured by Mehr and Biondi[16] and Alge et al.,[17] respectively. The associated branching ratios for the N_2^+ and NO^+ recombination reactions are $a_1 = 1.86$[18] and $a_2 = 0.76$.[19] In addition to Reactions (4) through (7), minor sources of $N(^2D)$ considered are the charge exchange reactions of N_2^+ with O[20] and N^+ with O_2[21,22]

$$N_2^+ + O \rightarrow N(^2D) + NO^+ \tag{8}$$

$$N^+ + O_2 \rightarrow N(^2D) + O_2^+ \quad . \tag{9}$$

Nitrogen atoms are also subject to quenching by other species which compete with Reactions (1) and (2) in the production of NO

$$N(^2D) + N_2 \rightarrow N(^4S) + N_2 \tag{10}$$

$$N(^2D) + O \rightarrow N(^4S) + O \tag{11}$$

$$N(^2P) + O \rightarrow N(^2D) + O \tag{12a}$$

$$N(^2P) + O \rightarrow NO^+ + e_s \quad . \tag{12b}$$

The quenching rates of Reactions (10)-(12)[6,23] are slow on the time scale of the EXCEDE III measurements in comparison to the efficient quenching of $N(^2D)$ and $N(^2P)$ by secondary electrons,[24] which results from the large density of secondary electrons created by the ionization rates achieved in the experiment

$$N(^2D) + e_s \rightarrow N(^4S) + e_s' \tag{13}$$

$$N(^2P) + e_s \rightarrow N(^4S,^2D) + e_s' \quad . \tag{14}$$

In addition to collisional quenching, $N(^2D)$ and $N(^2P)$ can undergo radiative relaxation

$$N(^2D) \rightarrow N(^4S) + h\nu \tag{15}$$

$$N(^2P) \rightarrow N(^2D,^4S) + h\nu \quad . \tag{16}$$

Since the N atom production from direct electron impact excitation and recombination reactions depends on the low energy secondary electron spectra, it is important that the histogram treatment retain the major features of the secondary electron spectra. Secondary electrons are formed via collisional ionization of $M(= N_2, O_2, \text{ or } O)$

$$e_p + M \rightarrow e_p + e_s + \text{products} \quad . \tag{17}$$

The nascent secondary electron energy distribution resulting from (17) is that given by Opal et al.,[25] which then relaxes by collisions with major species

$$e_s + M \rightarrow e_s' + M^* \tag{18}$$

and

$$e_s + M \rightarrow e_s' + e_s'' + M^+ \tag{19}$$

as well as electron-electron collisions

$$e_s + e_s' \rightarrow e_s'' + e_s''' \tag{20}$$

where the primes refer to secondary electrons in different energy bins. The ion production rates from Reaction (17) are related to the ion pair production rate via the expressions given by Rees

and Jones.[26] The rate constants for Reactions (18) and (19) were taken from the reviews of Itikawa et al.[27,28] for N_2 and O_2 and Itikawa and Ichimura[29] for O.

One of the most important inputs to the model is the electron beam characteristics, i.e., the radial profile of the ion-pair production rate. Historically, the electron deposition information has been deduced from the N_2^+ first negative 3914 Å emission, where it is assumed that there are 14.1 N_2^+ ions created for each 3914 Å photon.[26] Therefore, the beam ion pair production rate profiles used in the current model are based on an analysis of the 3914 Å data by Rieder et al.[2] The N_2^+ production rate, $P(N_2^+)$, is related to the total ion pair production rate, P_{ion}, by

$$P(N_2^+) = \frac{0.92[N_2]}{1.15[N_2]+1.5[O_2]+0.56[O]} P_{ion}$$

where the numerical factors in the expression represent the relative ionization cross sections for N_2, O_2, and O.[26] Using the atmospheric profile appropriate for the EXCEDE III experiment, the relative production rate of N_2^+ ions is approximately independent of altitude (ranging from 0.60 at 95 km to 0.62 at 115 km).

Representative predictions of the production and destruction rates for $N(^2D)$ and $N(^2P)$ are presented in Figures 1 through 4 for an altitude of 115 km. The electron beam ion pair production rate is represented by a generalized Gaussian function[2] with a peak ion pair production rate of 1.6×10^{11} ion pairs/cm^3-s and a full width at half maximum of 14 ms.
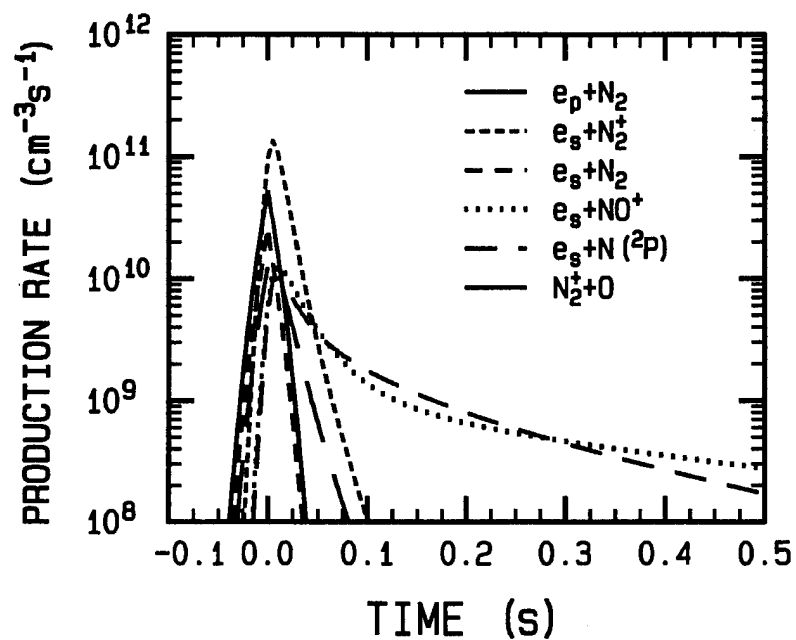
Figure 1. Major Processes for the Production Rate of $N(^2D)$ at 115 km.
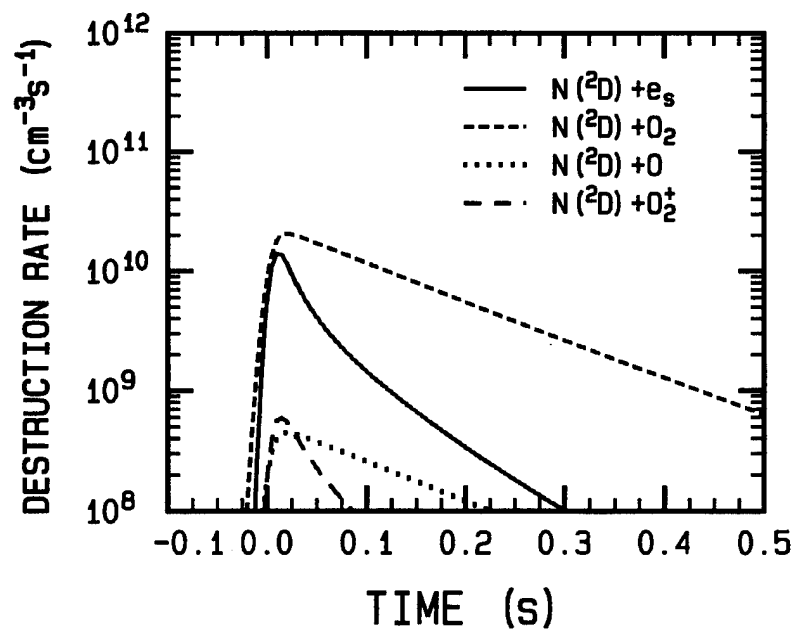

Figure 2. Major Processes for the Destruction Rate of $N(^2D)$ at 115 km.
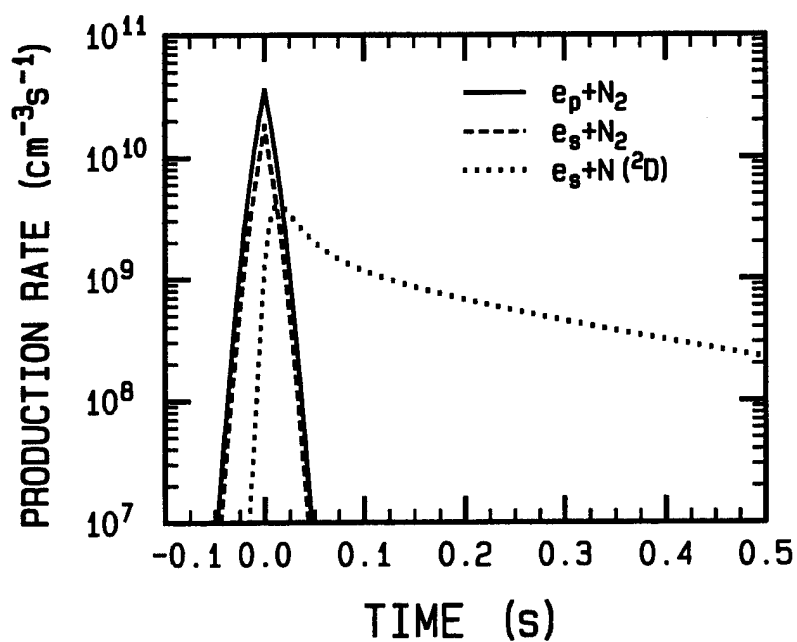
7

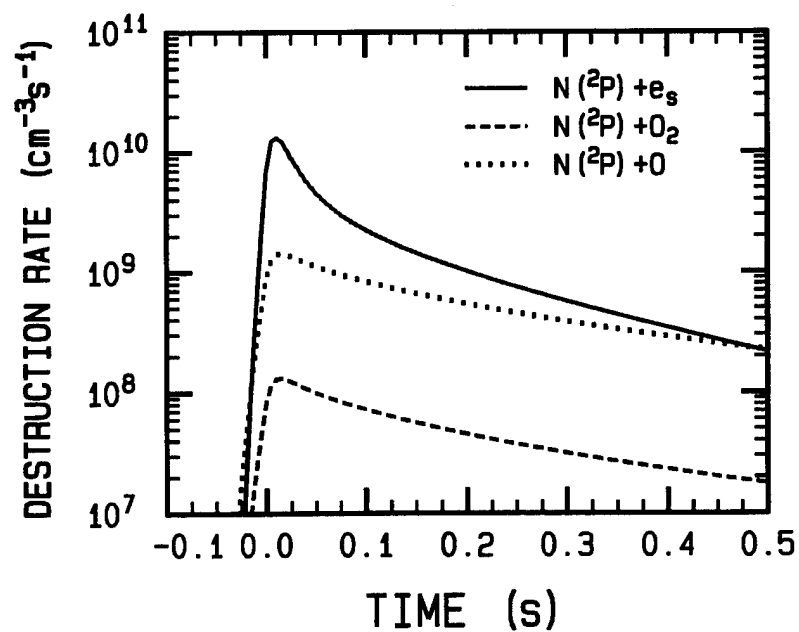**Figure 3.** Major Processes for the Production Rate of $N(^2P)$ at 115 km.

Figure 4. Major Processes for the Destruction Rate of $N(^2P)$ at 115 km.

8

4. COMPARISON OF DATA WITH THE KINETICS MODEL

The chemical kinetics mechanism described previously has been incorporated into the EXCEDE chemical kinetics data base. The resultant data base contains 6703 reactions and energy transfer processes. The chemical kinetics equations are integrated using Gear's method for stiff differential equations[30] as a function of time for a specified electron beam ion-pair production rate and altitude. The atmospheric profiles for N_2, O_2, and O were obtained from the MSISE-90 atmospheric model[31] for the geophysical parameters appropriate to the EXCEDE III experiment.

The geometry of the flight experiment, which includes the trajectory of the gun module, the geomagnetic azimuth and dip angles, and the viewing geometry of the 3466 Å visible spectrometer and 5200 Å photometer on the sensor module, has also been incorporated in the model. The time-dependent nitrogen atom number densities are integrated along the instrument line-of-sight to obtain the column densities as a function of time. The resultant column densities are then integrated over the 6° FOV of the instruments for comparisons with the column densities obtained from 3466 Å and 5200 Å data.

To illustrate the electron beam energy deposition throughout the EXCEDE flight, the total number of ion pairs produced by the electron beam is shown as a function of mission elapsed time (or altitude) in Figure 5. The number of ion pairs was obtained by integrating the observed 3914 Å scanning photometer data along the component of gun vehicle velocity vector perpendicular to the magnetic field lines. The maximum number of ion pairs are created near 102 km on upleg, where, due to the near zero velocity across the field lines, the atmosphere is dosed for nearly 0.5 seconds. The average electron-deposition time, which is simply the root mean square electron beam diameter divided by the velocity across the field lines, is shown in Figure 6. As altitude increases, the number of ion pairs produced decreases due to the shorter deposition times (i.e., the velocity across the field lines is increasing with altitude), see Figure 6. On downleg, the number of ion pairs again increases as altitude decreases, although the total number of ion pairs created is substantially less on downleg than on upleg. This effect is due to the atmosphere being irradiated by the electron beam for times up to a factor of 50 longer on upleg than on downleg, again as shown in Figure 6. The two data points at approximately 114 and 113 km are about 75% of the expected beam power output due to beam load faults.

9

The comparisons of the $N(^2D)$ and $N(^2P)$ column densities obtained from the 5200 Å and 3466 Å data with the model predictions which have been integrated along the line-of-sight and integrated over the sensor field-of-view are shown in Figures 7 and 8, respectively.

The agreement between the model predictions and data is excellent on both upleg and downleg for the $N(^2D)$ measurements. The altitude dependence of the $N(^2D)$ column density measurement, which looks 18° into the afterglow, is controlled by quenching of $N(^2D)$ by secondary electrons with increasing importance of the $N(^2D)+O_2$ reaction near 100 km. On upleg, the largest discrepancy between the model and data is at 109 and 111 km on upleg, which is not understood, although it is likely related to the uncertainty in the secondary electron quenching rate of $N(^2D)$. The differences between upleg and downleg $N(^2D)$ column densities simply reflect the differences the ion pair production rate, although the ratio of upleg to downleg $N(^2D)$ column densities is less sensitive to ion pair production rate due to the significant quenching of $N(^2D)$ and the fact that the primary production process for $N(^2D)$ is recombination of secondary electrons with N_2^+. The production rate of $N(^2D)$ from recombination roughly increases as the square root of the ion pair production rate.

The comparison of the model predictions with the 3466 Å data shown in Figure 8 indicate that the $N(^2P)$ chemistry is not as well established as the $N(^2D)$ chemistry. This comparison would indicate that the assumed production rate of 0.22 $N(^2P)$/ion pair used in Reaction (4b) is approximately a factor of 2 low. Since the total production rate of N atoms is fairly well established, increasing the rate for Reaction (4b) by a factor of 2 would imply that only $N(^2P)$ is produced by dissociation of N_2 by primary electrons. Such a modification in the $N(^2D)/N(^2P)$ relative production rate from Reaction (4) would not significantly alter the excellent agreement between the predictions and the 5200 Å data since the major production mechanism for $N(^2D)$ is the recombination of N_2^+ with secondary electrons, Reaction (6), as shown in Figure 1. Furthermore, the increase in $N(^2P)$ would provide more $N(^2D)$ due to the increased quenching rate from Reaction (14).
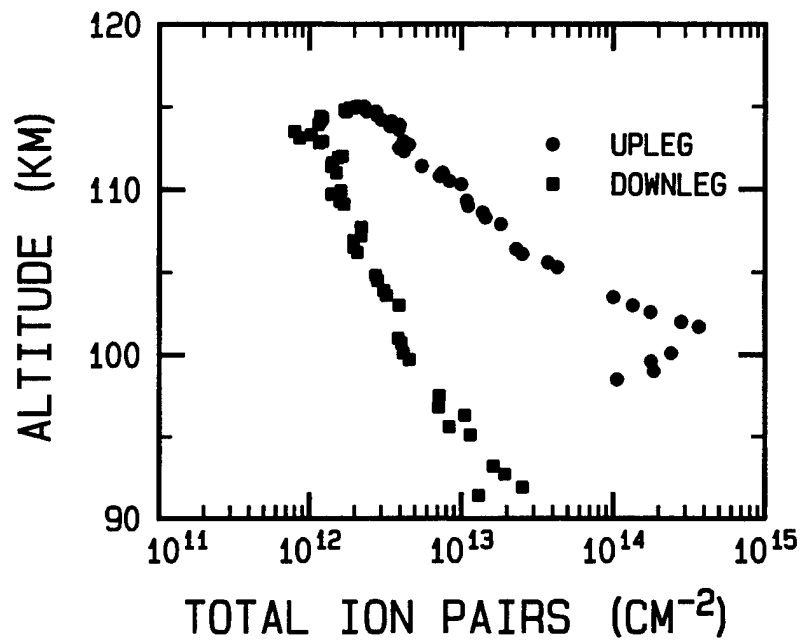
Figure 5. Total Number of Ion Pairs Along the Line-of-Sight as a Function of Mission Elapsed Time for the EXCEDE III Experiment.
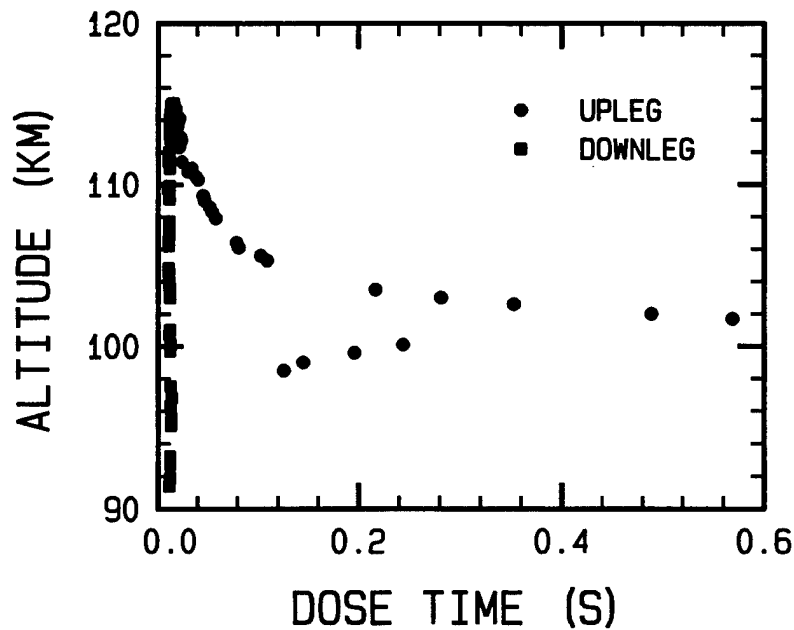

Figure 6. Calculated Dose Time as a Function of Mission Elapsed Time for the EXCEDE III Experiment.
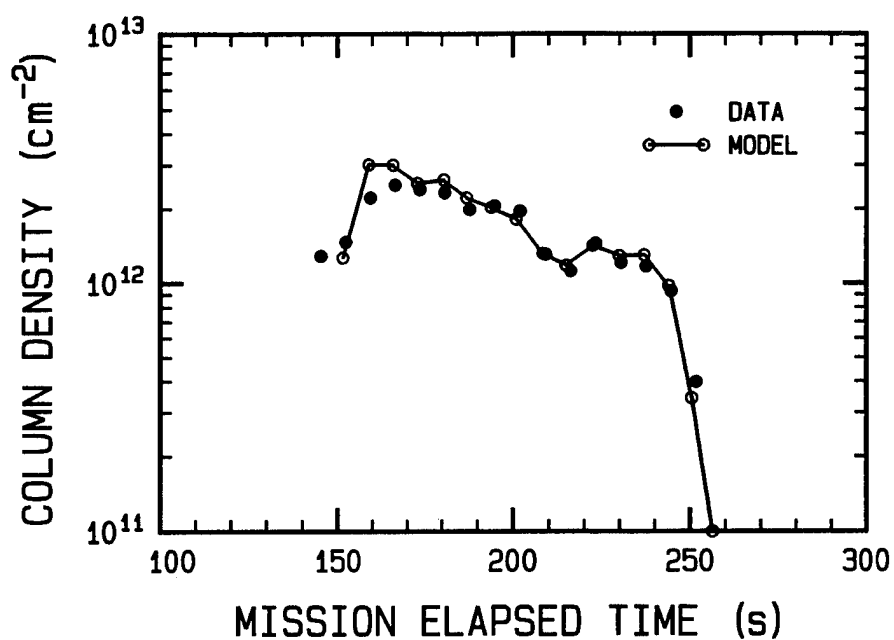
11

Figure 7. Comparison of the Time Dependence of the Calculated N(^{2}D) Column Density (o) with the 5200 Å Photometer Data (●).
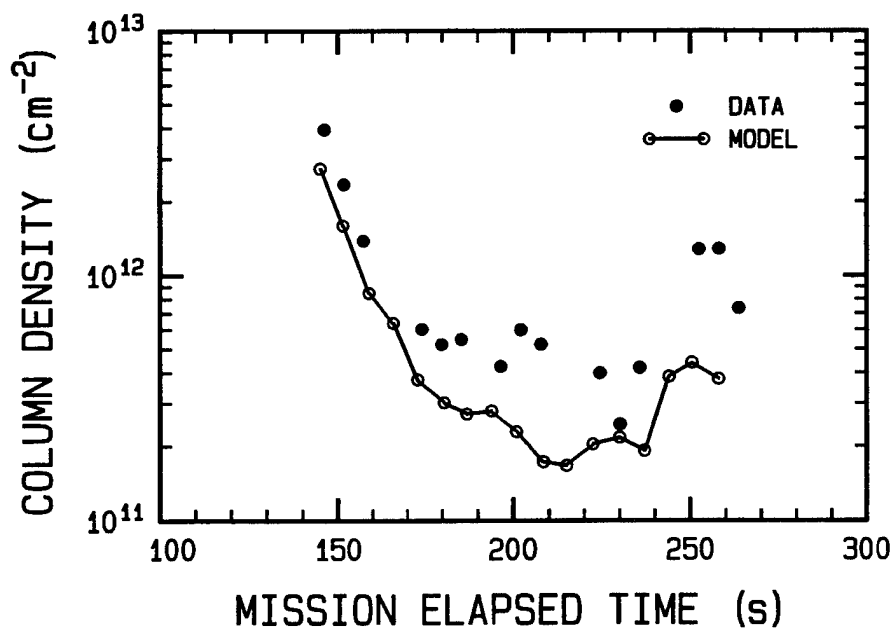

Figure 8. Comparison of the Calculated Time Dependence of the N(^{2}P) Column Density (o) with the 3466 Å Spectrometer Data (●).

5. SUMMARY

The EXCEDE III experiment has provided quantitative characterization of the $N(^2D)$ 5200 Å and $N(^2P)$ 3466 Å emissions resulting from the irradiation of the lower thermosphere (90-115 km) by an intense electron beam. A detailed chemical kinetics model indicates that the $N(^2D)$ emission can be quantitatively explained by assuming accepted production rates of $N(^2D)$ and N_2^+ created by the electron beam dissociation, consistent with previous auroral models. Using the previous estimate of 0.22 $N(^2P)$ per ion pair[14] from electron dissociation of N_2 results in a model prediction which is approximately 50% below the data, in disagreement with previous analyses of $N(^2P)$ auroral and dayglow emission.[14,32,33] However, it should be recalled that the EXCEDE III measurement of $N(^2P)$ was <u>not</u> made under steady state conditions, which are appropriate to the atmospheric observations. The present analysis would imply that the amount of $N(^2P)$ from N_2 dissociation should be about a factor of 2 greater than previously assumed or an additional source of $N(^2P)$ exists for intense electron beams such as that used in EXCEDE III.

6. REFERENCES

1. S. A. Rappaport, R. J. Rieder, W. P. Reidy, R. L. McNutt, Jr., J. J. Atkinsom, and D. E. Paulsen, "Remote X Ray Measurements Of The Electron Beam From The EXCEDE III Experiment," J. Geophys. Res., 98, 19093-19098 (1993).

2. R. J. Reider, R. L. McNutt, S. A. Rappaport, "Characterization Of The Energy Deposition Produced By The Primary Electron Beam On The EXCEDE III Experiment," Visidyne Rep. VI-2067, 32 pp., Visidyne, Inc., Burlington, MA (1993), PL-TR-93-2132(I), ADA274453.

3. O. Ashihara and K. Takayanagi, "Velocity Distribution Of Ionospheric Low-Energy Electrons," Planet. Space Sci., 22, 1201-1217 (1974).

4. M. Martinez-Sanchez, W. Cheng, D. Dvore, and M. S. Zahniser, "Electron Energy Distribution From Intense Electron Beams In The Upper Mesosphere And Lower Thermosphere," J. Geophys. Res., 97, 1363-1375 (1992).

5. J.-C. Gérard, "Thermospheric Odd Nitrogen," Planet. Space Sci., 40, 337-353 (1992).

6. L. G. Piper, "The Reactions Of $N(^2P)$ With O_2 And O," J. Chem. Phys., 98, 8560-8564 (1993).

7. J. P. Kennealy, F. P. Del Greco, G. E. Caledonia, and B. D. Green, "Nitric Oxide Chemiexcitation Occurring In The Reaction Between Metastable Nitrogen Atoms And Oxygen Molecules," J. Chem. Phys., 69, 1574-1584 (1978).

8. W. T. Rawlins, M. E. Fraser, and S. M. Miller, "Rovibrational Excitation Of Nitric Oxide In The Reaction Of O_2 With Metastable Atomic Nitrogen," J. Phys. Chem., 93, 1097-1107 (1989).

9. R. D. Sharma, Y. Sun, and A. Dalgarno, "Highly Rotationally Excited Nitric Oxide In The Terrestrial Thermosphere," Geophys. Res. Letters, 20, 2043-2045 (1993).

10. V. I. Shematovich, D. V. Bisikalo, and J. C. Gérard, "Non Thermal Nitrogen Atoms In The Earth's Thermosphere 1. Kinetics Of Hot $N(^4S)$," Geophys. Res. Lett., 18, 1691-1694 (1991).

11. J. W. Duff, F. Bien, and D. E. Paulsen, "Classical Dynamics Of The $N(^4S) + O_2(X^3\Sigma_g) \rightarrow NO(X^2\Pi) + O(^3P)$ Reaction," Geophys. Res. Lett., 21, 2043-2046 (1994).

12. H. S. Porter, C. H. Jackman, and A. E. S. Green, "Efficiencies For Production Of Atomic Nitrogen And Oxygen By Relativistic Proton Impact In Air," J. Chem. Phys., 65, 154-167 (1976).

13. D. W. Rusch, J.-C. Gérard, S. Solomon, P. J. Crutzen, and G. C. Reid, "The Effect Of Particle Precipitation Events On The Neutral And Ion Chemistry Of The Middle Atmosphere-I. Odd Nitrogen," Planet. Space Sci., 29, 767-774 (1981).

14. E. C. Zipf, P. J. Espy, and C. F. Boyle, "The Excitation And Collisional Deactivation Of Metastable N(^{2}P) Atoms In Auroras," J. Geophys. Res., 85, 687-694 (1980).

15. D. Rapp, P. Englander-Golden, and D. D. Briglia, "Cross Sections For Dissociative Ionization Of Molecules By Electron Impact," J. Chem. Phys., 42, 4081-4085 (1965).

16. F. J. Mehr and M. A. Biondi, "Electron Temperature Dependence Of Recombination Of O_2^+ And N_2^+ Ions With Electrons," Phys. Rev., 181, 264-271 (1969).

17. E. Alge, N. G. Adams, and D. Smith, "Measurements Of The Dissociative Recombination Coefficients Of O_2^+, $NO^{+,}$ And NH_4^+ In The Temperature Range 200-600 K," J. Phys. B: At. Mol. Phys., 16, 1433-1444 (1983).

18. J. L. Queffelec, B. R. Rowe, M. Morlais, J. C. Gomet, and F. Vallee, "The Dissociative Recombination Of N_2^+(v=0,1) As A Source Of Metastable Atoms In Planetary Atmospheres," Planet. Space Sci., 33, 263-270 (1985).

19. D. Kley, G. M. Lawrence, and E. J. Stone, "The Yield Of N(^{2}D) Atoms In The Dissociative Recombination Of NO^+," J. Chem. Phys., 66, 4157-4165 (1977).

20. D. L. McFarland, D. L. Albritton, F. C. Fehsenfeld, E. E. Ferguson, and A. L. Schmeltekopf, "Energy Dependence And Branching Ratio Of The N_2^+ + O Reaction," J. Geophys. Res., 79, 2925-2926 (1974).

21. D. Smith, N. G. Adams, and T. M. Miller, "A Laboratory Study Of The Reactions Of N^+, N_2^+, N_3^+, N_4^+, O^+, O_2^+, And NO^+ Ions With Several Molecules At 300 K," J. Chem. Phys., 69, 308-318 (1978).

22. M. A. Smith, V. M. Bierbaum, and S. R. Leone, "Infrared Chemiluminescence From Vibrationally Excited NO^+: Product Branching In The N^++O_2 Ion-Molecule Reaction," Chem. Phys. Letters, 94, 398-403 (1983).

23. C. Fell, J. I. Steinfeld, and S. Miller, "Quenching Of N(^{2}D) By O(^{3}P)," J. Chem. Phys., 92, 4768-4777 (1990).

24. K. A. Berrington and P. G. Burke, "Effective Collision Strengths For Forbidden Transitions In e-N And e-O Scattering," Planet. Space Sci., 29, 377-381 (1981).

25. C. B. Opal, W. K. Peterson, and E. C. Beaty, "Measurements Of Secondary-Electron Spectra Produced By Electron Impact Ionization Of A Number Of Simple Gases," J. Chem. Phys., 55, 4100-4106 (1976).

26. M. H. Rees and R. A. Jones, "Time Dependent Studies Of The Aurora-II. Spectroscopic Morphology," Planet. Space Sci., 21, 1213-1235 (1971).

27. Y. Itikawa, M. Hayashi, A. Ichimura, K. Onda, K. Sakimoto, K. Takayanagi, M. Nakamura, H. Nishimura, and T. Takayanagi, "Cross Sections For Collisions Of Electrons And Photons With Nitrogen Molecules," J. Phys. Chem. Ref. Data, 15, 985-1010 (1986).

28. Y. Itikawa, A. Ichimura, K. Onda, K. Sakimoto, K. Takayanagi, Y. Hatano, M. Hayashi, H. Nishimura, and S. Tsurubuchi, "Cross Sections For Collisions Of Electrons And Photons With Oxygen Molecules," J. Phys. Chem. Ref. Data, 18, 23-42 (1989).

29. Y. Itikawa and A. Ichimura, "Cross Sections For Collisions Of Electrons And Photons With Atomic Oxygen," J. Phys. Chem. Ref. Data, 19, 637-651 (1990).

30. C. W. Gear, Numerical Initial Value Problems in Ordinary Differrential Equations, Prentice-Hall, Englewood Cliffs, NJ (1971).

31. A. E. Hedin, "Extension Of The MSIS Thermosphere Model Into The Middle And Lower Atmosphere," J. Geophys. Res., 96, 1159-1172 (1991).

32. J.-C. Gérard and O. E. Harang, "Metastable $N(^2P)$ Atoms In The Aurora," J. Geophys. Res., 85, 1757-1761 (1980).

33. M. R. Torr, D. G. Torr, and P. G. Richards, "$N(^2P)$ In The Dayglow: Measurement And Theory," Geophys. Res. Lett., 20, 531-534 (1993).